【Article】

Thermal Structure of Steady Vortices on the Earth-like and the Sun-like Atmospheres

TAKAHASHI Koichi

Abstract : The temperature distributions within steady vortices are determined via. the thermal diffusion equation by assuming that the steady flow of viscous fluid is maintained by a supply of heat. The boundary-free Burgers vortex is examined first, and, together with exact solutions, eight types of physically acceptable temperature distribution are numerically found. Next, a vortex between two horizontal boundaries is examined by a truncated Fourier expansion approximation. Non-trivial solutions are shown to exist that have correspondence to such phenomena as the temperature anomalies observed in typhoons on the earth and in the transition region above the solar chromosphere.

Key words : vortex ; temperature ; heat conduction ; typhoon ; solar atmosphere

1. Introduction

There exist a large number of flows analytically determined by the Navier-Stokes equation and the continuity equation. Among them, steady flows of viscous fluid are of particular interest because not only of their physical reality but also of the fact that, in spite of their dissipative nature, their steadiness is unaltered in the course of time. In order for a steady flow of viscous fluid be possible, when no external body force is brought into operation, some other physical elements must be active which the NS equations and the continuity equation alone cannot capture. One likely candidate may be heat that is continuously supplied by the environments. In this case, the fluid will build up a structure of temperature distribution characteristic of the flow.

In this paper, we would like to focus our attention specifically to vortices because of their intriguing flow structures and ubiquity in nature. In fact, vortices exist over very wide range of spatial scale, ranging from the nano-sized ones in inviscid superfluid droplet (Gomez et al. 2014) to the galaxy-size of the order of 10^5 light years (see, e.g., Binney and Tremaine 2008). On the other hand, there are several simple vortices whose mathematical structures are well-known and are regarded to be prototypes of vortices in nature as long as the velocity structures are concerned (see, e.g., Drazin and Riley

2006). They have one feature in common : the kinetic energy along the stream line is not conserved under the absence of external force. It is natural to attribute the variance of the kinetic energy to the variance of thermal energy. However, the thermal structures of simple vortices have not been seriously explored so far despite the fact that vortices in nature are frequently driven by heat supply. We address a question : What thermal structures are realized in simple vortices and to what extent do the simple vortices simulate the thermal properties of real vortices ?

The familiar vortices that are driven by heat are typhoons. It has been observationally confirmed that they often possess a temperature anomaly at the centre in the form of warm core (Hawkins and Rubsam 1968 ; Halverson et al. 2006) due to the convergence and convection of humid air at the sea surface. The solar atmosphere is also a place where vortices of large scales may be expected to be created due to abundance of heat flow. One peculiarity observed there is the precipitous rise of temperature in a relatively very thin region above the chromosphere (Carlsson and Stein 2004 ; Avrett and Loeser 2008). It is not known whether simple vortices are consistent to these phenomena. The primary purpose of the present paper is to look into the latent thermal structures of the simple vortices on the basis of the law of heat diffusion. We would like to successively compare the results with the phenomena in the earth's and the solar atmospheres.

The temperature distribution in a simple vortex was analytically studied long ago by Rott (1959) for the Burgers vortex (Burgers 1948). He solved the equation that expresses the balance between the heat diffusion and, instead of advection, the entropy change in a flow with high Reynolds numbers, thereby finding solutions with radial coordinate dependence only. Obviously, such an approach is insufficient for comparing the theoretical consequences with the natural three-dimensional phenomena we are interested in.

Preliminary numerical calculations of temperature distributions for simple vortices in incompressible fluid had been done for axisymmetric configuration, with an indication that the tendency of the temperature anomaly in typhoon was nicely reproduced by taking the thermodynamical effect of shear (Takahashi 2015a, 2016 (Erratum)). This result strongly suggests that the continuing supply of (latent) heat from the 'environment' can be a key mechanism to maintain the vortex motion as is the case for typhoon (Hawkins and Rubsam 1968 ; Halverson et al. 2006 ; Charney and Eliassen 1964 ; Ooyama 1966). The aim of this paper is to elaborate the previous calculation with an additional scope of applying the method to understand the thermal property of an analogous system, i.e., the solar atmosphere.

In the next section, we summarize the physics of the heat diffusion in fluid. In sec. 3 and 4, we

apply the heat diffusion equation to two kinds of steady vortices and put the law of heat diffusion into tractable forms for those vortices. One is the Burgers vortex as the representative example of having no boundaries and the other is a vortex with two horizontal boundaries. In sec. 5, the temperature distributions are calculated and their implications on phenomena of real atmospheres in the earth and the sun are discussed. Sec. 6 is devoted to summary and remarks.

2. Heat diffusion equation in fluid — review —

In this section, we obtain the equation for the temperature distribution in steady flow. We start from the heat diffusion equation in a flow described by the velocity field $\boldsymbol{u}(\boldsymbol{x})$

$$\rho \frac{dq}{dt} = \sum_{\alpha,\beta} p_{\alpha\beta} \frac{\partial u_\alpha}{\partial x_\beta} + \sum_{\beta} \frac{\partial}{\partial x_\beta} \left(\kappa \frac{\partial T}{\partial x_\beta} \right). \tag{2.1}$$

Here, q is the thermal energy per unit mass, ρ the density, $p_{\alpha,\beta}$ the stress tensor, T the temperature, and κ the heat conductivity. The first term on the r.h.s. of (2.1) is the work done on the fluid volume by the pressure, and the second term is the heat transfer to the volume based on Fourier's law of thermal conduction. The heat is also advected by the flow and the total derivative in time on the l.h.s. is given by $d/dt = \partial/\partial t + \boldsymbol{u} \cdot \nabla$. (2.1) expresses the energy conservation in the flow. For details, see, e.g., Bittencourt (2004). Phase transitions and the heat generations associated to it are disregarded, although these are essential elements that govern the dynamics of typhoon (Charney and Eliassen 1964 ; Ooyama 1966). This means that, concerning a vortex in earth's atmosphere, we regard the vapour as an effective environment for air flow.

The stress tensor is expressed as

$$p_{\alpha\beta} = -\left(p + \frac{2}{3} \mu \nabla \cdot \boldsymbol{u} \right) \delta_{\alpha\beta} + 2\mu s_{\alpha\beta}, \tag{2.2a}$$

$$s_{\alpha\beta} = \frac{1}{2} \left(\frac{\partial u_\alpha}{\partial x_\beta} + \frac{\partial u_\beta}{\partial x_\alpha} \right), \tag{2.2b}$$

where p is the pressure, μ the viscosity and $s_{\alpha\beta}$ the rate-of-strain tensor.

Now, we express (2.1) in the cylindrical coordinate (r, θ, z) by using the identity

$$\sum_{\alpha,\beta}\frac{\partial u_\beta}{\partial x_\alpha}\frac{\partial u_\alpha}{\partial x_\beta}=2(\partial_r\mu_r)^2+2\frac{(\partial_\theta u_\theta+u_r)^2}{r^2}+2(\partial_z u_z)^2$$
$$+\left(\partial_r u_\theta+\frac{\partial_\theta u_r-u_\theta}{r}\right)^2+(\partial_r u_z+\partial_z u_r)^2+\left(\frac{1}{r}\partial_\theta u_z+\partial_z u_\theta\right)^2. \tag{2.3}$$

From (2.1) ~ (2.3), we have the general expression of the law of the heat generation

$$\frac{dq}{dt}=\frac{1}{\rho}\sum_{\alpha=r,\theta,z}\frac{\partial}{\partial x_\alpha}\left(\kappa\frac{\partial T}{\partial x_\alpha}\right)-\left(\frac{p}{\rho}+\frac{2}{3}\nu\nabla\cdot\boldsymbol{u}\right)\nabla\cdot\boldsymbol{u}+2\nu\left[(\partial_r u_r)^2+\frac{1}{r^2}(\partial_\theta u_\theta+u_r)^2+(\partial_z u_z)^2\right]$$
$$+\nu\left[\left(\partial_r u_\theta+\frac{\partial_\theta u_r-u_\theta}{r}\right)^2+(\partial_r u_z+\partial_z u_r)^2+\left(\frac{1}{r}\partial_\theta u_z+\partial_z u_\theta\right)^2\right], \tag{2.4}$$

where $\nu\equiv\mu/\rho$ is the kinematic viscosity, which is assumed to be constant throughout this paper.

For the axisymmetric case, terms involving ∂_θ are dropped and (2.4) simplifies as

$$\frac{dq}{dt}=\frac{1}{\rho}\nabla\cdot(\kappa\nabla T)-\frac{p}{\rho}\nabla\cdot\boldsymbol{u}+\nu\Phi, \tag{2.5}$$

where Φ is given by

$$\Phi=\frac{4}{3}\left((\partial_r u_r)^2+\frac{u_r^2}{r^2}+(\partial_z u_z)^2-\frac{u_r}{r}\partial_r u_r-\frac{u_r}{r}\partial_z u_z-\partial_r u_r\partial_z u_z\right)$$
$$+\left(\partial_r u_\theta-\frac{u_\theta}{r}\right)^2+(\partial_r u_z+\partial_z u_r)^2+(\partial_z u_\theta)^2. \tag{2.6}$$

In case the fluid is incompressible, u_r and u_z are related by $\nabla\cdot\boldsymbol{u}=\partial_r u_r+u_r/r+\partial_z u_z=0$ and Φ will be dominated by the contributions from shear. Hereafter, we shall call Φ the shear function.

When the phase transition is absent, the heat generation will directly give rise to the temperature change via.

$$\delta q=c_{\mathrm{h}}\delta T, \tag{2.7}$$

where c_{h} is the heat capacity under the circumstances the fluid is placed. It will generally depend on p and T, although, for simplicity, we assume that it is a constant of the order of the Boltzmann constant, k_{B}, for each degree of freedom of constituent particles. Since the fluid is in a steady state, from (2.5) and (2.7), we finally have

$$\frac{1}{\rho}\nabla\cdot(\kappa\nabla T)-c_{\mathrm{h}}\boldsymbol{u}\cdot\nabla T=\frac{p}{\rho}\nabla\cdot\boldsymbol{u}-\nu\Phi. \tag{2.8}$$

This equation describes how the stress contributes to the thermal structure of a steady flow. In the following sections, we apply (2.8) to incompressible vortices (i.e., $\nabla\cdot\boldsymbol{u}=0$) with simplification that ρ, κ, c_{h} and ν are constant. The temperature is a passive scalar whose thermal diffusivity is given by

$$\lambda = \frac{\kappa}{\rho c_{\mathrm{h}}}. \tag{2.9}$$

Rott (1959) utilized a temperature equation similar to (2.8) to determine the temperature distribution in a linear vortex. Unfortunately, his equation is not correct because of an overestimation of the pressure contribution. We will come back to this point in the next section.

3. Application of (2.8) to the Burgers vortex

The Navier-Stokes equation for the steady axisymmetric vortex assumes invariance under the transformation $\nu \to -\nu$, $u_r \to -u_r$, $u_z \to -u_z$, $u_\theta \to u_\theta$. The velocity field

$$\boldsymbol{u} = (\nu u_{r1}(r, z), u_\theta(r, z), \nu u_{z1}(r, z)) \tag{3.1}$$

for a steady, axisymmetric and unbounded vortices is of the simplest one that fulfils the above invariance. u_{r1}, u_θ and u_{z1} are independent of ν and obeys the equations

$$u_{r1}''' + \left(\frac{2}{r} - u_{r1}\right)u_{r1}'' - \left(\frac{1}{r^2} - \frac{u_{r1}}{r} - u_{r1}'\right)u_{r1}' + \frac{u_{r1}}{r^3} + \frac{2{u_{r1}}^2}{r^2} = 4k^2, \tag{3.2a}$$

$$u_{z1} = -\frac{z}{r}(ru_{r1})' \equiv -x(r)z, \tag{3.2b}$$

$$u_\theta = \frac{\Gamma}{2\pi r}\int_0^r dr r e^{\int^r dr' u_{r1}(r')}. \tag{3.2c}$$

Here, k and Γ are arbitrary real constants. The prime stands for a derivative in r. These equations are derived by substituting (3.1) to the Navier-Stokes equation and matching the coefficients of each order of ν. The condition $u_{z1} = 0$ at $z = 0$ has been posed in (3.2b), although the origin of z-axis is arbitrary. The pressure is determined by the balance equation with the centrifugal force.

The continuous series of solutions to (3.2a) ~ (3.2c) has been known to exist (Takahashi 2014). By 'continuous', we mean that the azimuthal component u_θ with fixed k and Γ changes its functional form continuously in accordance with the change of the third integration constant. The solutions can be classified into three types. The type I involving Burgers solution (Burgers 1948) consist of one cell. The type II involves Sullivan solution (Sullivan 1959) and consists of two cells. The type III consists of three cells. In this section, we take the Burgers vortex as the example to which (2.8) is applied.

The Burgers vortex, which situates at the edge of the type I family (Takahashi 2004), is given by

$$u_{r1} = -kr, \tag{3.3a}$$

$$u_{z1} = 2kz, \tag{3.3b}$$

$$u_{\theta 0} = \frac{\Gamma}{2\pi r}\left(1 - e^{-kr^2/2}\right). \tag{3.3c}$$

k (=(vortex's characteristic size)$^{-2}$) and Γ (= circulation at infinity) are arbitrary constant.

The shear function (2.6) becomes

$$\Phi(r) = \left(\partial_r u_\theta - \frac{u_\theta}{r}\right)^2 + 12\nu^2 k^2, \tag{3.4a}$$

$$\Phi(0) = \Phi(\infty) = 12\nu^2 k^2. \tag{3.4b}$$

(3.4b) means that the stress at the stagnation points is equal to the one at $r=\infty$. The Reynolds number of the vortex is the order of Γ/ν. The Reynolds number of the typical typhoon is the order of 10^{12} or greater. For such vortices, Φ is dominated by u_θ and the last term in (3.4a) is safely dropped. The heat diffusion equation (2.8) is expressed as

$$\frac{\kappa}{\nu\rho}\nabla^2 T = c_{\mathrm{h}} u_{r1}\partial_r T + c_{\mathrm{h}} u_{z1}\partial_z T - \Phi. \tag{3.5}$$

Here, Φ is given by (3.4a) with $12\,\nu^2 k^2$ being dropped. The corresponding equation that Rott (1959) derived by assuming that T is a function of r only is

$$\frac{1}{\rho r}\frac{d}{dr}\left(\kappa r \frac{dT}{dr}\right) = u_r\left(c_{\mathrm{h}}\frac{dT}{dr} - \frac{u_\theta^2}{r}\right) - \nu\left(\frac{du_\theta}{dr} - \frac{u_\theta}{r}\right)^2. \tag{3.6}$$

The first term on the r.h.s. expresses the contribution from entropy, in which the second term $-u_\theta^2/r$ has emerged from the variation of the pressure. This term therefore implies that the decrease in the pressure has been used for solely absorbing heat. However, in the Navier–Stokes equation, the local force due to the pressure gradient affects both accelerating the fluid element and the dissipation of energy by stress. The inconsistency inherent in (3.6) is manifested by considering the inviscid limit that allows no energy dissipation. Suppose that an incompressible and inviscid fluid is bounded by isothermal surface. Since the heat is not internally generated, the temperature is same everywhere. Taking the limit $\nu \to 0$ and $dT/dr \to 0$ simultaneously in (3.6), we have $u_r u_\theta^2 \to 0$. Now, recalling that k in (3.3) is arbitrary, let us scale k as k/ν before taking the limit. Then, from (3.3a) and (3.3c), we have $u_r u_\theta^2 = \nu u_{r1} u_{\theta 0}^2 \to -k(\Gamma/2\pi)^2/r \neq 0$ in the same limit. This is a contradiction. By these reasoning, we adopt (3.5) or (2.8) in the following analyses.

4. Application of (2.8) to a vortex with two parallel boundaries

In this section we consider a vortex with two parallel plane boundaries perpendicular to the z-axis as a model of air flow in typhoon bounded by the sea surface and the tropopause. Of course, the dynamics of real typhoon involves complexities due to such important ingredients as Coriolis force, humidity and condensation, rain-bands, eye-walls of clouds and so on. We neglect these elements and focus ourselves on the air-flows of vortex to which heat is transferred from the lower boundary. We also neglect the friction at boundaries because the thickness of the boundary layer is several hundred meters, which may be small enough as compared to the height $h \approx 15$ km of the tropopause (Cherney 1947 ; Franklin et al. 2003).

Steady axisymmetric vortex with boundaries will not exist in case no-slip condition is imposed, the external force is conservative or the fluid is barotropic (Proudman 1916 ; Taylor 1917 ; Takahashi 2015b). As usual in solving the Navier-Stokes equation, the pressure is allowed to have spatial dependences, too. Namely, the fluid will not be barotropic. No-slip condition on boundaries will not be imposed, too.

For the present purpose, it will be convenient to subject the physical quantities to the ν-expansion together with to a truncated Fourier expansion in z. Then we assume the following forms for velocity, pressure and temperature :

$$u_{r1}(r, z) = a_1(r)\cos(k_1 z) + a_2(r)\cos(k_2 z), \tag{4.1a}$$

$$u_{z1}(r, z) = b_1(r)\sin(k_1 z), \tag{4.1b}$$

$$u_\theta(r, z) = c_0(r) + c_1(r)\cos(k_1 z), \tag{4.1c}$$

$$p_i(r, z) = \pi_{i,n}(r)\cos(k_n z), \quad i = 0, 2, \tag{4.1d}$$

$$T(r, z) = \tau_0(r) + \tau_1(r)\cos k_1 z + \tau_2(r)\cos k_2 z, \tag{4.1e}$$

where $k_n = n\pi/h$, $n = 1, 2$. These expansions are the simplest ones that are compatible with the invariance of the Navier-Stokes equation for a steady and axisymmetric flow under $z \to -z$, $u_z \to -u_z$. For large Reynolds numbers, the shear function is dominantly contributed from u_θ as

$$\begin{aligned}\Phi &= \left(\partial_r u_\theta - \frac{u_\theta}{r}\right)^2 + (\partial_z u_\theta)^2 \\ &= \left(c_0' - \frac{c_0}{r}\right)^2 + \frac{1}{2}\left[\left(c_1' - \frac{c_1}{r}\right)^2 + k_1^2 c_1^2\right] + 2\left(c_0' - \frac{c_0}{r}\right)\left(c_1' - \frac{c_1}{r}\right)\cos k_1 z \\ &\quad + \frac{1}{2}\left[\left(c_1' - \frac{c_1}{r}\right)^2 - k_1^2 c_1^2\right]\cos 2k_1 z. \end{aligned} \tag{4.2}$$

By substituting (4.1a ~ e) and (4.2) to the Navier-Stokes equation, the mass conservation and the heat diffusion equation, we have

$$a_1''+\left(\frac{1}{r}-\frac{a_2}{2}\right)a_1'-\left(\frac{1}{r^2}+\frac{a_2'}{2}+k_1^2\right)a_1=-\frac{k_2b_1}{2}a_2, \tag{4.3a}$$

$$a_2''+\frac{a_2'}{r}-\left(\frac{1}{r^2}+k_2^2\right)a_2=\frac{a_1'+k_1b_1}{2}a_1, \tag{4.3b}$$

$$b_1''+\frac{b_1'}{r}-k_1^2b_1=-\frac{k_1}{\rho}\pi_{2.1}, \tag{4.3c}$$

$$c_0''+\frac{c_0'}{r}-\frac{c_0}{r^2}=\frac{1}{2}a_1\left(c_1'+\frac{c_1}{r}\right)-\frac{k_1}{2}b_1c_1, \tag{4.3d}$$

$$c_1''+\left(\frac{1}{r}-\frac{a_2}{2}\right)c_1'-\left(\frac{1}{r^2}+\frac{a_2}{2r}+k_1^2\right)c_1=\left(c_0'+\frac{c_0}{r}\right)a_1, \tag{4.3e}$$

$$a_1'+\frac{a_1}{r}+k_1b_1=0, \tag{4.4}$$

$$\tau_0''+\frac{1}{r}\tau_0'-\frac{\rho c_h\nu}{2\kappa}(a_1\tau_1'+a_2\tau_2'-k_1b_1\tau_1)=-\frac{\rho\nu}{\kappa}\left[\left(c_0'-\frac{c_0}{r}\right)^2+\frac{1}{2}\left(c_1'-\frac{c_1}{r}\right)^2+\frac{1}{2}k_1^2c_1^2\right], \tag{4.5a}$$

$$\tau_1''+\frac{1}{r}\tau_1'-k_1^2\tau_1-\frac{\rho c_h\nu}{\kappa}\left(a_1\tau_0'+\frac{a_1\tau_2'+a_2\tau_1'-k_2b_1\tau_2}{2}\right)=-\frac{2\rho\nu}{\kappa}\left(c_0'-\frac{c_0}{r}\right)\left(c_1'-\frac{c_1}{r}\right). \tag{4.5b}$$

With the truncated Fourier series (4.1), it is impossible for the equation (2.8) to hold for all modes exactly. In deriving the above equations, therefore, we gave precedence to the lower modes with τ_2 being determined by the boundary condition, i.e., $T(r,0)=T_0(r)$, or, from (4.1e),

$$\tau_0(r)+\tau_1(r)+\tau_2(r)=T_0(r). \tag{4.6}$$

Let us seek the simplest solution by positing

$$a_1(r)=a_{11}r,\ a_2(r)=a_{21}r, \tag{4.7a}$$

$$b_1(r)=\pi_{2.1}/\rho k_1\equiv b, \tag{4.7b}$$

where a_{11}, a_{21} and b are constant provided that these satisfy (see (4.3a), (4.3b) and (4.4))

$$a_{11}a_{21}+k^2a_{11}=kba_{21}, \tag{4.8a}$$

$$a_{11}^2+kba_{11}=-8k^2a_{21}, \tag{4.8b}$$

$$2a_{11}+kb=0, \tag{4.8c}$$

with $k\equiv k_1$. Nontrivial roots of (4.8) are given by

$$\frac{a_{11}}{k^2}=\mp\sqrt{\frac{8}{3}},\quad \frac{a_{21}}{k^2}=\frac{1}{3},\quad \frac{b}{k}=\pm2\sqrt{\frac{8}{3}}. \tag{4.9}$$

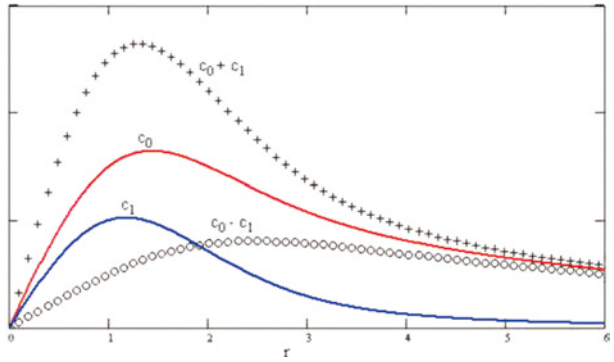

Fig. 1 c_0 and c_1 as functions of r. The units of abscissa and ordinate are arbitrary. c_0+c_1 and c_0-c_1 are $u_{\theta 0}$ at $z=0$ and h, respectively.

We adopt the upper signs in (4.9), which stand for a vortex that swirls inward, rises to higher elevations and then swirls outward. Then c_0 and c_1 that are determined from (4.3d) and (4.3e) are shown in Fig. 1. c_0 and c_1 behave linearly near $r=0$. At long distances, they decay as $1/r$ and $1/r^3$, respectively. Being constructed from these c_0 and c_1, $u_{\theta 0}$ at $z=h$ has the same sign as the one at $z=0$. If the Coriolis force were taken into account, there would exist points where $u_{\theta 0}$ changes its sign just like the real typhoons.

Now that the velocity field has been determined, the temperature will be found by solving (4.5a) and (4.5b) with the boundary condition (4.6).

5. Temperature distributions in vortices

5.1 Solutions to the homogeneous equation for Burgers vortex

Temperature T as the solution to (3.5) is given by a sum of the solution of the homogeneous equation, T_{homo}, and the particular solution, T_{pat}, to the inhomogeneous equation. We first look for T_{homo} which is generally z-dependent.

Separating the variables by

$$T_{\text{homo}} = f(r)g(z)+T_0, \tag{5.1}$$

(2.8) or (3.5) with Φ being omitted reduces to two ordinary differential equations

$$f''+\left(\frac{1}{r}+\frac{\nu k}{\lambda}r\right)f'+Cf=0, \tag{5.2a}$$

$$g''-\frac{2\nu k}{\lambda}zg'-Cg=0, \tag{5.2b}$$

where C is an arbitrary constant that gives a length scale of variation by $|C|^{-1/2}$ for small $\nu k/\lambda$. λ was defined by (2.9). We are interested in the case $C \neq 0$.

It is not difficult to find f and g for the Burgers vortex. We define a dimensionless parameter α by

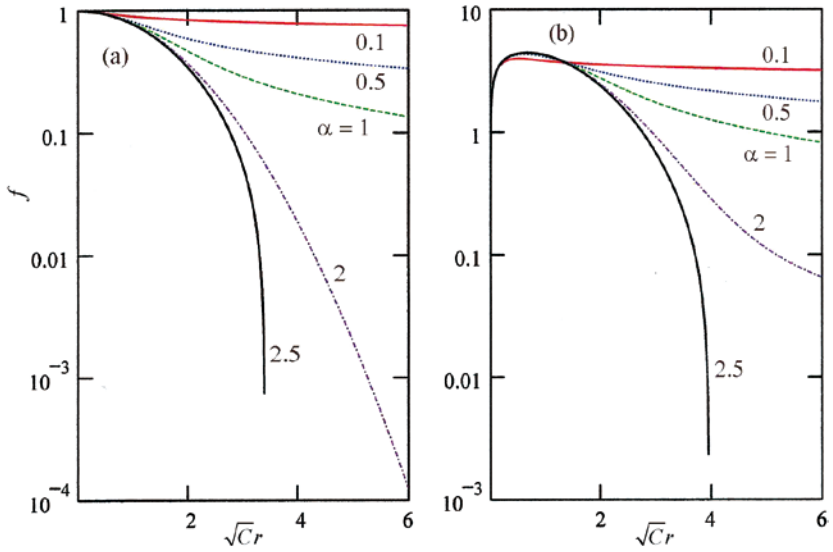

Fig. 2 f for positive α as obtained by solving (A4a) in Appendix A. Normalization is arbitrary. The value of α is indicated nearby each curve. The behaviours of f near $r=0$ are conventionally chosen as (a) : $1-r^2/4$, (b) : $(1-r^2/4)\ln r$. C is an additional free parameter that is involved in equations (5.2). (k is determined by (5.3)). The units of abscissa and ordinate are arbitrary.

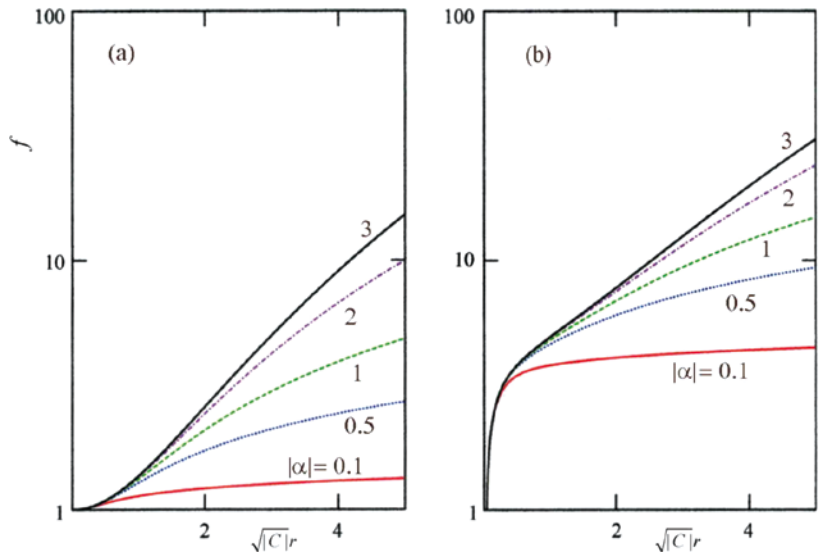

Fig. 3 f for negative α. Normalization is arbitrary. The numbers in the figures denote $|\alpha|$. The distinction between panels (a) and (b) is same as in Fig. 2.

$$\alpha = \frac{\lambda C}{\nu k} = \frac{C}{k\mathrm{Pr}} \tag{5.3}$$

with k being the parameter used to specify the velocity field in (3.4). $\mathrm{Pr} = \nu/\lambda$ is the Prandtl number. The functional forms of f and g are determined essentially by α. (5.3) implies that α has the same sign as C. The solutions to (5.2a) and (5.2b) are shown in Fig. 2-3 and Fig. 4-5, respectively, for several values of α. See Appendix A for the details of deriving and solving (5.2).

The functions f depicted in Fig. 2-3 exhibit power law behaviour $r^{-\alpha}$ at long distances. The rate of change of f becomes larger with $|\alpha|$. The function g depicted in Fig. 4-5 exhibit either power law decays with r or exponential growth. The eight possible combinations of f and g are given by [Fig. 2, Fig. 4] and [Fig. 3, Fig. 5]. Notice that in the latter combination the exact solution for $\alpha = -2$ exists :

$$f = 1 + |C| r^2/4, \quad g = z. \tag{5.4}$$

We will employ (5.4) in later numerical calculations.

Next, we seek a particular solution T_{pat} to the inhomogeneous equation (3.5). That Φ is a function of r only may suggest T_{pat} also to be a function of r only. Then (3.5) takes a form

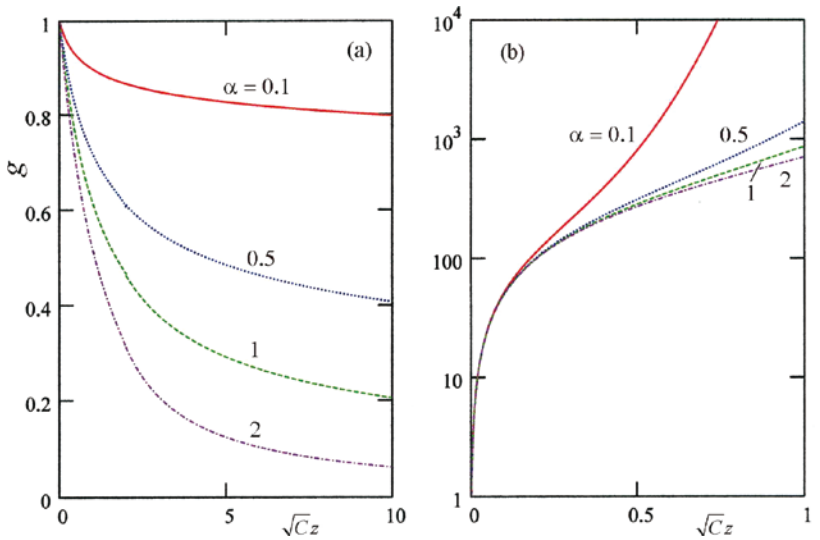

Fig. 4 g for positive α. g's are obtained by solving (A4b) in Appendix A. Normalization is arbitrary. Conventional boundary conditions are (a) : $g(0) = 1$. $g'(0)$ were appropriately chosen so as for $g(z)$ not to diverge at large z. (b) : $g(10^{-3}) = 1$, $g'(0^{-3}) = 10^3$. The value of α is indicated nearby each curve. The units of abscissa and ordinate are arbitrary. Note the difference in the scale of abscissa of Fig. 3 and Fig. 4, indicating the necessity of very fine tunings of initial conditions to obtain non-divergent solutions depicted here.

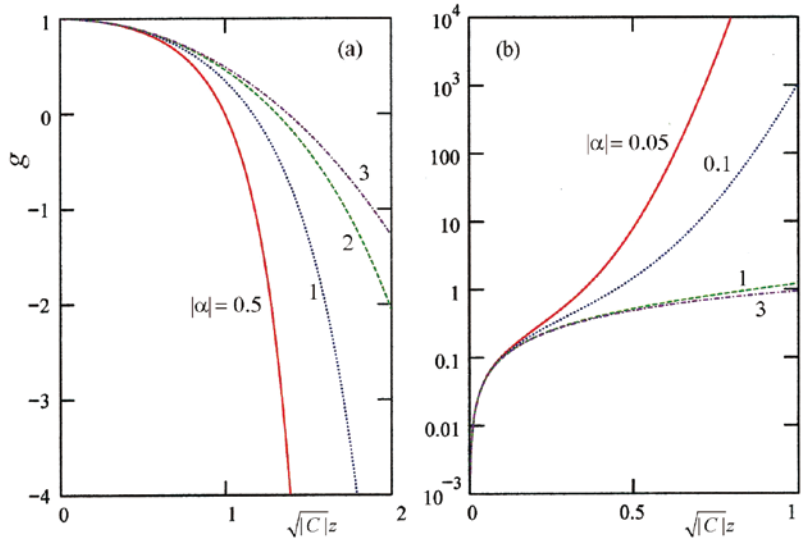

Fig. 5　g for negative α. Normalization is arbitrary. Conventional boundary conditions are (a) : $g(0)=1$, $g'(0)=0$, (b) : $g(0)=0$, $g'(0)=1$. The value of $|\alpha|$ is indicated nearby each curve. The units of abscissa and ordinate are arbitrary.

$$T_{\mathrm{pat}}''+\left(\frac{1}{r}+\frac{\nu k}{\lambda}r\right)T_{\mathrm{pat}}'=-\frac{\nu\rho}{\lambda}\Phi. \tag{5.5}$$

The analytic expression of T_{pat} is given by

$$T_{\mathrm{pat}}(r)=T_1-\frac{\nu\rho}{\lambda}\int_0^r e^{-Cr'^2/2\alpha}\frac{dr'}{r'}\int_0^{r'}\Phi(r'')e^{Cr''^2/2\alpha}r''\,dr'', \tag{5.6}$$

where T_1 is a constant. Note that T_{pat} does not affect the z-dependence of the solution.

5.2　Temperature for Burgers vortex

Before solving the temperature equation in its full form, let us evaluate the relative importance of the shear term Φ in (5.5). Keeping the atmospheres of the earth and the sun in mind, we can crudely estimate the r.h.s. of (5.5). It turns out to be the order of 10^{-6} K・m^{-2} for the earth atmosphere and 10^{-11} K・m^{-2} for the solar atmosphere. On the other hand, the l.h.s. of (5.5) may be estimated by kT_{obs}, where T_{obs} is the observed typical temperature and $k^{-1/2}$ is the characteristic linear size of the vortex, thereby obtaining $kT_{\mathrm{obs}}\sim 10^{-6}$ K・m^{-2} for the earth and $10^{-8}\sim 10^{-6}$ K・m^{-2} for the sun. Therefore, concerning the sun, we can neglect the shear term in (5.5) and the temperature is given by the homogeneous solution $f(r)g(z)$. See Appendix B for the details of these estimations.

T_{pat} for the earth-like atmosphere in the sense mentioned above is shown in Fig. 6. Notice that it is virtually constant in the region designated. This implies that the appreciable temperature change, if

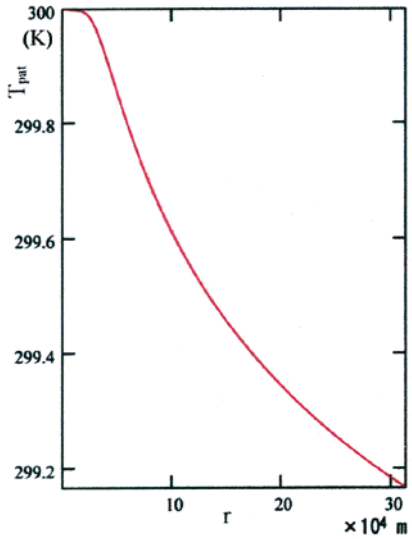

Fig. 6 Particular solutions (5.6) for Burgers vortex. Boundary conditions are $T_{pat}(0)=300$ K, $dT_{pat}/dr(0)=0$. For the employed physical constants and parameters, see Appendix B.

any, will be realized by the homogeneous solution.

We examine the implications of the solutions on the phenomena in the earth-like and the sun-like atmospheres.

Earth-like atmosphere (One boundary at $z=0$) : The values of such physical quantities as the temperature, the density and the viscosity are taken as of the same orders of those of the air on the earth. Moisture is entirely disregarded. In the circumstances on the earth, T_{pat} will not generally be neglected (see Appendix B), so that the solution must be sought as a linear combination of T_{homo} and T_{pat} as

$$T = T_{pat} + T_{homo}, \quad T_{homo} = -5\times 10^{-6} f(r)g(z) + \text{constant}. \tag{5.7}$$

T_{pat} has been presented in Fig. 6. For simplicity, we choose the exact solution (5.4) for T_{homo}. This means that the boundary conditions

$$T(r, z=0) = T_{pat}(r) + \text{constant}, \tag{5.8a}$$

$$T(r, z\to\infty) \to -\infty. \tag{5.8b}$$

are imposed. An example of the temperature distribution thus obtained is presented in Fig. 7.

We define the temperature anomaly at a given height z by

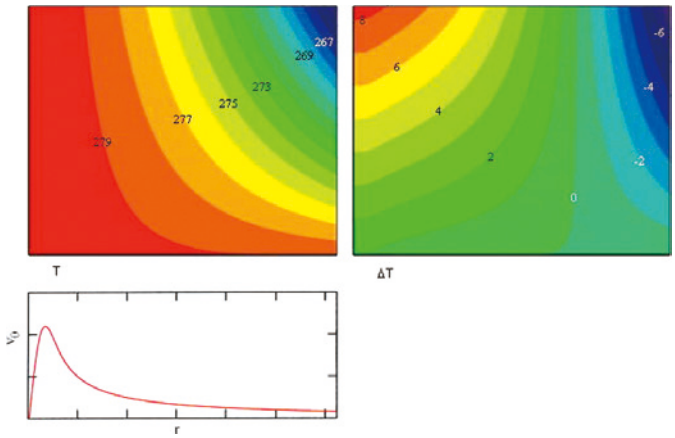

Fig. 7　Upper left panel : T (arbitrary constant can be added.) ; Upper right panel : ΔT ; abscissas : r with max(r)＝310 km, ordinates : z with max(z)＝15 km. Lower panel : u_θ for the Burgers vortex. max(u_θ)＝30 m・s^{-1}, α＝0.1 and $C^{-1/2}$＝45 km. Temperatures are plotted as contours of the spacing of 1 K and are also shown as colours ranging from red (high) through purple (low). Values of T and ΔT are given on some contours.

$$\Delta T(r, z) = T(r, z) - \frac{2\pi}{S}\int T(r, z) r dr, \tag{5.9}$$

where S is the area of the maximum horizontal circle in which the calculation is made. $\Delta T(r, z)$ is also shown in Fig. 7.

The temperature is dependent on both r and z. The lower as well as central part is warmer than the exterior or higher region because of the choice (5.7) for T_{homo}, thereby forming a 'warm core' of ΔT in the higher elevation around the symmetry axis. If the sign of T_{homo} were inverted, the opposite situation would result.

Nontrivial thermal structures have turned out to be inherent generally in the Burgers vortex. However, an obvious deficit of applying it to the earth's atmosphere lies in that the Burgers vortex is unbounded. The vortex with two boundaries, whose mathematical analysis has been given in sec. 4, will be considered in the next subsection.

Sun-like atmosphere : The solar surface is a good place where the model of the Burgers vortex can be applied. The surface and outer regions of the sun are conventionally divided into the photosphere, the chromosphere and the corona, which are differentiated from each other by spectroscopy. See, e.g., Audouze (1994). The temperature in the sun's atmosphere shows a sudden increase, from 10^4 K to 10^6 K, in the transition region as thin as 10^3 km or less between chromosphere and corona. Ionizations and recombinations of hydrogen and other elements, chromospheric heating and associated

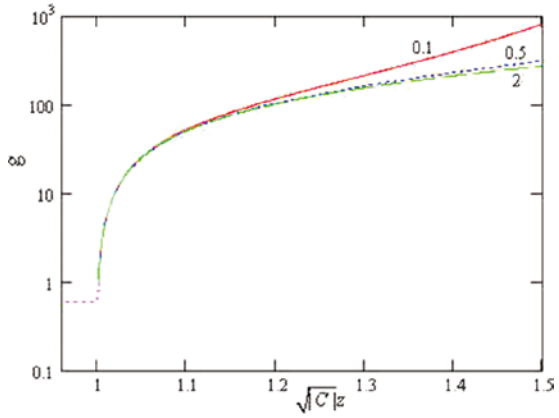

Fig. 8 Steeply rising $g(z)$ for positive α : $\alpha = 0.1$ (solid curve), 0.5 (dotted curve), 2 (dashed curve). The functions in $\sqrt{C}\,z \geq 1$ are smoothly connected with the solution that is obtained with $\alpha = 0.0016$ and is almost flat in lower region (dotted curve in the lower left). These solutions are obtained under the conditions $g(C^{-1/2}) = 1$, $dg/dz\,|_{C^{1/2}z=1} = 500C^{1/2}$. The origin of z is arbitrary.

energy flow may be responsible for this anomalous phenomenon (see, e.g., Carlson and Stein 2004 ; Avrett et al. 2008). We here notice that the function $g(z)$ introduced by (5.1) also has a transient region where steep increases are observed as are depicted in Fig. 3(b), Fig. 4(b) or Fig. 5(b). Choosing the parameters appropriately, this behaviour can be smoothly connected to other solution beneath the transient region. This smooth connection results in an almost flat behaviour of g in the lower region, as is shown in Fig. 8.

As was already argued, for understanding the temperature variation in the solar atmosphere, the homogeneous solution $f(r)g(z)$ will be sufficient if the solutions of these types mentioned above are applied. On the other hand, if we require that the variation over the radial direction, i.e., the direction parallel to the plane tangential to the solar sphere, is not large, then, from Fig. 2 and Fig. 3, $\alpha < 0.1$ may be favourable. Adopting for the Prandtl number the value $\mathrm{Pr}_{\mathrm{sun}} = \nu_{\mathrm{sun}}/\lambda_{\mathrm{sun}} \approx 14$ (see Appendix B), we have a condition $\alpha = (1/\mathrm{Pr}_{\mathrm{sun}})(C/k) \approx 0.07C/k < 0.1$ (α has been defined by (5.3)). Thus the order of the scale parameter $C^{-1/2}$ in the figures may be same as or larger than that of horizontal scale $k^{-1/2}$ of the vortex (see (3.3c)), which can be chosen as 10^7 m if the vortex is associated to the sun spot as is argued in Appendix B. From. Fig. 8, the thickness δ of the zone within which g increases one hundred times larger with altitude is given by $C^{1/2}\delta \approx 0.1$, or $\delta \approx 0.1/k^{1/2} \approx 10^3$ km. Instead of the sun spots, the granules of 10^6 m in size may be possible to provide the scale $k^{-1/2}$ of the vortices. In this case, we have $\delta \approx 10^2$ km. These estimations seem not inconsistent with the observation.

The Burgers vortex with no azimuthal shear must have a very weak swirling on the solar surface, provided that the Lorentz force is balanced with the magnetic pressure gradient in plasma (see Appendix B). In this case, the motion of the fluid will look like the Burgers flow with no azimuthal component of the velocity.

If the present scheme of the vortex interpretation for the rapid temperature change above the chromosphere is applied also to the inside of the chromosphere and the function g is extrapolated to smaller z, then a drastic change in the value of α defined by (5.3) from 0.1 to 0.002 is necessary. One interpretation for this situation is that the Prandtl number is two order of magnitude larger for the chromosphere than for the transition region. However, this is unlikely because the heat conductivity in the chromosphere will be larger. Therefore, the decrease of C will be responsible for the decreases of α. The physical meaning of this phenomenon is unclear.

5.3 Vortex with two boundaries

Finally, we calculate the temperature of the vortex with two horizontal boundaries separated each other by the distance h. As the boundary condition, the surface temperature $T_0(r)$ at $z=0$ of a rather arbitrarily chosen form is adopted :

$$T_0(r)=\frac{T_{S0}}{1+(r/2)^2}. \tag{5.8}$$

This functional form models the high temperature of a local sea surface on which typhoon is born.

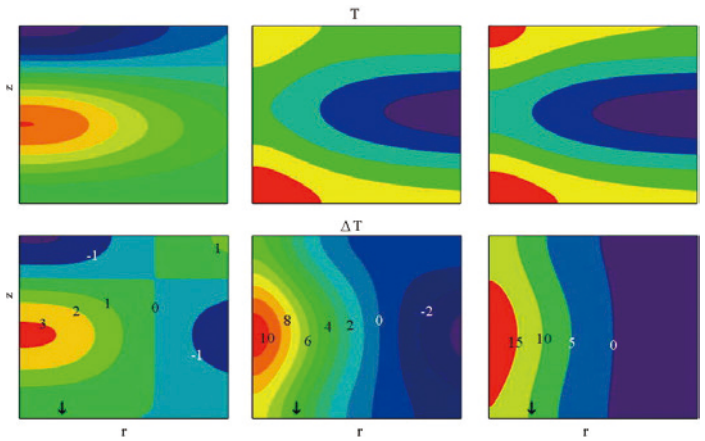

Fig. 9　T (upper panels) and ΔT (lower panels) for the vortex with two horizontal boundaries that are $h=15$ km apart. For T, an arbitrary constant can be added. The arrows indicate the position of the maximum of u_θ at $z=0$. Some values of $\Delta T(r,z)$ are indicated on contours. $T_{S0}=0.1$ K, 10 K and 20 K from left to right. The spacing of neighbouring contours in the graphs of ΔT is 1 K for $T_{S0}=0.1$ K and $T_{S0}=10$ K, while it is 5 K for $T_{S0}=20$ K. For azimuthal velocity, we set $\max(u_\theta(r,z=0))=40\,\mathrm{m}\cdot\mathrm{s}^{-1}$.

(4.5a) and (4.5b) are solved by employing the velocity field determined in sec. 4. The particular solutions for three cases $T_{S0}=0.1$, 10, 20 K are shown in Fig. 9.

The maximum temperature differences, $\max(T)-\min(T)$, are 11, 28 and 57 K for $T_{S0}=0.1$, 10 and 20 K, respectively. As is expected, the temperature difference gets larger with the surface temperature difference. Other characteristic features of each case are briefly summarized below.

i) $T_{S0}=0.1$: This is as the representative of the cases of zero or extremely small temperature differences in the lower boundary. The maximum temperature is at the middle altitude on the symmetry axis. Thus a warm ball is formed. The lowest temperature is at the centre of the upper boundary. The temperature anomaly ΔT is also largest at the middle point of the axis. ΔT is smallest at the centre of the upper boundary, i.e., a cold core exists there.

ii) $T_{S0}=10$: The maximum temperature is at the centre of the lower boundary. As the altitude gets higher along the axis, the temperature gets lower and reaches a minimum and then again becomes higher. The lowest temperature is at the outermost between two boundaries. Thus a *cold belt* surrounds the axis. The largest ΔT is at the middle point of the axis, which is again akin to the so called 'warm core' in typhoon. The smallest ΔT is at the farthest point from the axis. At a given altitude, the temperature anomaly is largest at the axis.

iii) $T_{S0}=20$: The situations are generally similar to the case of $T_{S0}=10$, except that the central temperature is higher.

The features summarized in i), ii) and iii), which are contrasted with the Burgers vortex discussed in the previous subsection, are quite similar to the observed warm core-pillar structure in typhoons (Hawkins and Rubsam 1968 ; Halverson et al. 2006), although the height of the warm core calculated here is lower than that of the real typhoon. The warm core already exists when the temperature on the lower boundary is uniform. Comparing the cases of $T_{S0}=10$ and 20 with $T_{S0}=0.1$, we may conclude that the existence of a locally warm region in the sea surface is responsible for the formation of the distinct warm core-pillar, albeit a warm lump in T is also formed on the upper boundary.

6. Summary and remarks

The temperatures within vortices were calculated by employing the law of heat transfer, assuming that the vortices are maintained by heat supply. The boundary-free Burgers vortex and the one with two boundaries were chosen for the calculations. For these cases, significant temperature variances

over the vortex were observed.

Eight types of physically meaningful temperature variations were found for the Burgers vortex. The two of them seem to bear physical correspondences in nature, i.e., either to the solar-like or the earth-like atmospheres. In particular, a very slow variation followed by a steep rise of temperature with height found for the Burgers vortex is quite similar to that is actually occurring in the solar atmosphere. We may anticipate that the Burgers vortex will serve as a prototype of stellar atmosphere.

The vortex with two boundaries was found to be able to capture the qualitative characteristics of the thermal property observed in real typhoons. This result, somewhat amazing when we think of the simplest truncation method in the Fourier expansions utilized, suggests the significance of the boundary condition in understanding the temperature anomaly. In real typhoons, the condensation and precipitation in moist air are crucial in bringing about the peculiar thermal structure (Charney and Eliassen 1964 ; Sundqvist 1970 ; Nong and Emanuel 2003) because of the large specific heat of water. When the temperature at the lower boundary is almost uniform, the temperature first rises with the altitude and then decreases, so that the phase transition of moisture will take place near the upper boundary. On the contrary, when an appreciable lump of high temperature exists on the lower boundary, the temperature decreases at the middle point of the altitude and the liquefaction of moisture will take place around there. In both cases, the advection will shift the position of the warm core to higher elevation. What we have seen in the present work is that the warm core or warm pillar always exists in vortices of viscous fluid. Thus we can anticipate that the analogous thermal structure will exist in tornado, too.

The simple vortices discussed in this paper are lacking in many physical factors operating in forming the real atmosphere in nature, whose investigations require handling of large data on ingredients (See, e.g., Carlsson and Stein 2004 ; Avrett and Loeser 2008 for solar atmosphere, Ohno and Satoh 2015 for typhoon, together with references cited therein). Nevertheless, the thermal structure discussed in this paper is generic and must be heeded in studying vortices.

The gravity was totally neglected in this paper. This may be partly justified by the smallness of the change of gravity strength over the height we considered, as long as the fluid density depends only on z.

In this paper, it was elicited that temperature variations are generally inherent in the flows presented as the solution of the Navier-Stokes equation with absence of particular external force. Viscosity is known to vary with temperature. That temperature varies over vortex (or fluid) raises a question : Should the kinematic viscosity in the Navier-Stokes equation be treated as a function of temperature

when the scale of the vortex is large ? In other words, is the temperature or the kinematic viscosity really passive scalars ? This problem is worthy of future study.

Appendix A : Solution to the homogeneous equation

Omitting the source term in (3.5), we start with the static homogeneous equation

$$\frac{\kappa}{\nu\rho}\nabla^2 T_{\rm homo} - c_{\rm h} u_{r1}\partial_r T_{\rm homo} - c_{\rm h} u_{z1}\partial_z T_{\rm homo} = 0. \tag{A1}$$

u_{r1} and u_{z1} are given respectively by (3.3a) and (3.3b). Separating the variables, write

$$T_{\rm homo} = f(r)g(z) + T_0, \tag{A2}$$

where T_0 is a constant, and substitute (A2) to (A1) to obtain

$$\frac{\kappa}{\nu\rho}\frac{1}{rf}(rf')' - c_{\rm h}u_{r1}\frac{f'}{f} = -\frac{\kappa}{\nu\rho}\frac{g''}{g} + c_{\rm h}u_{z1}\frac{g'}{g} \equiv -\frac{\kappa}{\nu\rho}C. \tag{A3}$$

Here, the prime denotes a derivative with respect to the independent variable of each function. C is a constant. From (A2), we obtain a set of equations (5.2a) and (5.2b) in the text. α, being given by (5.3), and C must have the same sign. We consider two cases, $\alpha > 0, C > 0$ and $\alpha < 0, C < 0$, separately.

(1) $\alpha > 0, C > 0$

By scaling the variable by $r \to r/\sqrt{C}$ and $z \to z/\sqrt{C}$ and using (3.3), we rewrite (A3) as

$$f'' + \left(\frac{1}{r} + \frac{r}{\alpha}\right)f' + f = 0, \tag{A4a}$$

$$g'' - \frac{2}{\alpha}zg' - g = 0. \tag{A4b}$$

At infinity, f exhibits a power law behaviour for general α

$$f \to r^{-\alpha}, \quad r \to \infty, \tag{A5}$$

which means that the temperature becomes lower with the distances from the centre. This behaviour will dominate over the other possible one $f \to r^{-\alpha}\exp(-r^2/2\alpha)$.

Near $r = 0$, (A4a) allows two behaviours, ~ constant and ~ r. These initial behaviours yield the solutions consistent with the assumed asymptotic behaviour (A5), which are shown in Fig. 2 and Fig. 3 in the text for several values of α.

$\alpha = 2$ is a special value, for which the exact Gaussian solution is also found :

$$f(r) = e^{-Cr^2/4} \quad \text{for} \quad \alpha = 2. \tag{A6}$$

Another particular value of α is unity, for which the solution is generally written as

$$f(r)=e^{-Cr^2/4}\left(a_1 I_0(Cr^2/4)+a_2 K_0(Cr^2/4)\right),\quad \text{for } \alpha=1, \tag{A7}$$

where I_0 and K_0 are the modified Bessel functions of the first and the second kind, respectively. In this case, near $r=0$ and at large distances, f behaves as

$$f(r)\approx\left(1-\frac{Cr^2}{4}\right)\left[a_1+a_2\left(\ln 2-\gamma-\ln\frac{Cr^2}{4}\right)\right]\approx a_1+a_2\left(\ln 2-\gamma-\ln\frac{Cr^2}{4}\right),\quad \text{near } r=0, \tag{A8}$$

and

$$f(r)\to e^{-Cr^2/4}\left(a_1\frac{e^{Cr^2/4}}{\sqrt{\pi Cr^2/2}}+a_2\sqrt{\frac{\pi}{Cr^2/2}}\,e^{-Cr^2/4}\right)\to\frac{a_1}{r},\quad r\to\infty, \tag{A9}$$

respectively. γ is the Euler's constant. a_2 must be zero if the logarithmic singularity at $r=0$ is disfavoured, although there may be no reason for this choice because the logarithmic singularity at a point will not cause any difficulty in physical measurements.

Apart from the overall normalization, the limiting behaviours of g are of the following forms

$$g\approx 1+\frac{Cz^2}{2},\quad z-\left(\frac{1}{3\alpha}+\frac{1}{6}\right)Cz^3,\quad z\approx 0, \tag{A10a}$$

$$\to z^{-\alpha/2},\quad \frac{\alpha}{z}e^{Cz^2/\alpha},\quad z\to\infty. \tag{A10b}$$

The solutions that are finite or vanish at $r=0$ decay or grow rapidly at large z, respectively.

For $\alpha=2$, one can find one exact solution to (A4b)

$$g(z)=\sqrt{z}\;e^{Cz^2/2}K_{1/4}(Cz^2/2)\begin{cases}\approx 1+\dfrac{Cz^2}{2}, & z\approx 0,\\ \to e^{Cz^2}, & z\to\infty.\end{cases} \tag{A11}$$

where $K_{1/4}$ is the modified Bessel function of the second kind.

(2)　$\alpha<0, C<0$

As in the previous case, let us rewrite (A4a) in terms of the variable $r'=|C|^{1/2}r$ as

$$f''+\left(\frac{1}{r'}+\frac{r'}{|\alpha|}\right)f'-f=0. \tag{A12}$$

The asymptotic behaviour of f is again given by (A8) and now diverges at infinite distances. Near $r=0, f$ behaves as

$$f\sim 1+|C|r^2/4. \tag{A13}$$

The r.h.s. is exact for $\alpha=-2$.

We note that

$$g = z \tag{A14}$$

is also the exact solution for $\alpha = -2$. Generally the behaviour of g is given by

$$g \approx 1 - \frac{|C|z^2}{2}, \quad z + \left(\frac{1}{3|\alpha|} - \frac{1}{6}\right)|C|z^3, \quad z \approx 0, \tag{A15a}$$

$$\to z^{-|\alpha|/2}, \quad z^{-1}e^{-C_z^2/\alpha}, \quad z \to \infty. \tag{A15b}$$

Independent solutions for $\alpha < 0, C < 0$ are depicted in Fig. 4 and Fig. 5 in the text.

Appendix B : Physical parameters of the earth's and solar atmospheres

In this appendix, all the physical quantities are expressed in MKSA unit. The physical constants of the air on the earth are well determined. For the purpose of the order estimations, we adopt the following values : $\rho_E = 1\ \mathrm{kg \cdot m^{-3}}$, $c_{h,E} = 10^3\ \mathrm{J \cdot K^{-1} \cdot kg^{-1}}$, $\nu_E = 2\times10^{-5}\ \mathrm{m^2 \cdot s^{-1}}$, $\kappa_E = 2\times10^{-2}\ \mathrm{J \cdot m^{-1} \cdot s^{-1} \cdot K^{-1}}$, $\lambda_E = \kappa_E/(\rho_E c_{h,E}) \approx 2\times10^{-5}\ \mathrm{m^2 \cdot s^{-1}}$. The suffix 'E' (and 'S' below) stands for values for the earth's (and solar) atmosphere. These values give $\lambda_E/\nu_E \approx 1$. For the vortex parameters, we adopt $k_E = 10^{-8}\ \mathrm{m^{-2}}$, $\Gamma_E = 2\times10^6\ \mathrm{m^2 \cdot s^{-1}}$. From (3.4) and (3.5), the contribution of the shear function Φ_E to the thermal diffusion is given by $\nu\rho(\Gamma k/4\pi)^2/\kappa|_E = (\nu/\lambda)(\Gamma k/4\pi)^2 c_h|_E$ and is estimated as $2\times10^{-9}\ \mathrm{K \cdot m^{-2}}$. The typhoon's typical value of dT/dr is $10^{-4}\ \mathrm{K \cdot m^{-1}}$ (Halverson et al. 2006), so that the order of the remaining terms may be $k^{1/2}\,dT/dr \approx 10^{-8}\ \mathrm{K \cdot m^{-2}}$. Thus the Φ term will not be ignored.

The situation is subtle for the solar atmosphere. Besides, it is not known whether vortices are formed in the solar atmosphere or how large they are, if any. Various physical processes, e.g., excitations, dissociations and recombinations of atoms, excitations of collective motions and so on will affect the physical constants in thermo-fluid dynamics. Therefore, we stay at very rough order estimations. The relevant density, temperature and the heat capacity in the transition region are $\rho_S \approx 5\times10^{-10} \sim 5\times10^{-12}\ \mathrm{kg \cdot m^{-3}}$, $T_S \approx 10^4 \sim 3\times10^5\ \mathrm{K}$ and $c_{h,S} \approx 3\times10^4\ \mathrm{J \cdot K^{-1} \cdot kg^{-1}}$, respectively. The difference in temperature ΔT_S within the transition layer reaches as high as $3\times10^5\ \mathrm{K}$. According to the classical molecular kinematics, the kinematic viscosity will be corrected from the air value by a factor $(m_S/m_E)^{1/2}(T_S/T_E)^{1/2}/\{(\rho_S/\rho_E)(\sigma_S/\sigma_E)\}$, where m and σ are the representative mass of particles in the atmosphere and their collision cross section, respectively. Similarly, $\lambda_S = \kappa_S/(\rho_S c_{h,S}) \approx \lambda_E(m_S/m_E)^{-1/2}(T_S/T_E)^{1/2}/\{(\rho_S/\rho_E)(\sigma_S/\sigma_E)(c_{h,S}/c_{h,E})\}$ for the heat conductivity. Thus $\lambda_S/\nu_S \approx (\lambda_E/\nu_E)(m_E/m_S)(c_{h,E}/c_{h,H}) \approx \lambda_E/\nu_E$.

One candidate of the place where vortices are formed may be a strongly magnetized sunspot, whose

size is the order of 10^7 m, to which we equate $k_S^{-1/2}$. Assuming that the Lorentz force on the fluid moving with the azimuthal velocity u_θ is balanced with the gradient of the magnetic pressure $B_S^2/2\mu_0$, where μ_0 is the magnetic permeability of vacuum, then $eB_S u_\theta/m_S \approx \ell^{-1}(B_S^2/2\mu_0)/\rho_S$. Here, e is the electric charge of the proton, m_S the proton mass and ℓ the length scale of the gradient of the magnetic field. Using a value $B_S \approx 0.3$ tesla and writing $\ell = \beta k_S^{-1/2}$, we have $k_S^{-1/2} u_\theta \approx 2\times 10^6/\beta \mathrm{m}^2\cdot\mathrm{s}^{-1}$ and thus for the circulation, $\Gamma_S \approx 2\pi k_S^{-1/2} u_\theta \approx 10^7/\beta \mathrm{m}^2\cdot\mathrm{s}^{-1}$. With these values, $\Phi_S = \nu\rho(\Gamma k/4\pi)^2/k_S$ $\approx 2\times 10^{-21}/\beta^2 \mathrm{K}\cdot\mathrm{m}^{-2}$. On the other hand, in the transition region of the thickness $\delta \approx 3\times 10^2$ km, the laplacian term in (3.5) may give rise to a contribution $\delta^{-2}\Delta T_S \approx 3\times 10^{-6}\ \mathrm{K}\cdot\mathrm{m}^{-2}$. Thus, for reasonable values of β, Φ_S is extremely small as compared to the laplacian term and can be ignored.

References

Audouze J 1994, *The Cambridge atlas of astronomy* (Cambridge University Press).

Avrett E H and Loeser R 2008, Models of the solar chromosphere and transition region from SUMER and HRTS observations : Formation of the extreme-ultraviolet spectrum of hydrogen, carbon, and oxygen, *Astrophys. J. Suppl. Ser.* **175** 229.

Binney J and Tremaine S 2008, *Galactic Dynamics* (Princeton Univ. Press, Princeton).

Bittencourt J A 2004, *Fundamentals of plasma physics* (Springer, New York) Chap. 8.

Burgers J M 1948, A mathematical model illustrating the theory of turbulence, *Adv. Appl. Mech*. **1** 171.

Carlsson M and Stein R F 2004, Chromosperic heating and dynamics in *The solar-B mission and the forefront of solar dynamics : ASP Conf. Ser*. **325** 243.

Cherney J G 1947, The dynamics of long waves in a baroclinic westerly current, *J. Meteo.* **4** 135.

Charney J G and Eliassen A 1964, On the growth of the hurricane depression, *J. Atmos. Sci*. **21** 68.

Degiacomi C G, Kneubühl F K and Huguenin D 1985, *ApJ.* **298** 918.

Drazin P and Riley N 2006, The Navier-Stokes equation, A classification of flows and exact solutions, *London Math. Soc. Lec. Note Ser. 334* (Cambridge Univ.).

Franklin J L, Black M and Valde K 2003, GPS dropwindsonde wind profiles in hurricanes and their operational implications, *Wea. Forecasting* **18** 32.

Gomez L F, Ferguson K R, Cryan J P, Bacellar C, Tanyag R M P, Jones C, Schorb S, Anielski D, Belkacem A, Bernando C, Boll R, Bozek J, Carron S, Chen G, Delmas T, Englert L, Epp S W, Erk B, Foucar L, Hartmann R, Hexemer A, Huth M, Kwok J, Leone S R, Ma J H S, Maia F R N C, Malmerberg E, Marchesini S, Neumark D M, Poon B, Prell J, Rolles D, Rudek B, Rudenko A, Seifrid M, Siefermann K R, Sturm F P, Swiggers M, Ullrich J, Weise F, Zwart P, Bostedt C, Gessner O and Vilesov A F 2014, Shapes and vorticities of superfluid helium nanodroplets, *Science* **345** 906.

Halverson J B, Simpson J, Heymsfield G, Pirce H, Hock T and Ritchie L 2006, Warm core structure of hurricane Erin diagnosed from high altitude dropsondes during CAMEX-4, *J. Atmos. Sci*. **63** 301.

Hawkins H F and Rubsam D T 1968, Hurricane Hilda, 1964 II. Structure and budgets of hurricane on October 1, 1964, *Mon. Wea. Rev*. **96** 617.

Nong S and Emanuel 2003, A numerical study of the genesis of concentric eyewalls in hurricanes, *Q. J. R. Meteorol. Soc*. **129** 3323.

Ohno T and Satoh M 2015, On the warm core of a tropical cyclone formed near the tropopause, *J. Atmos. Sci*. **72** 551.

Ooyama K 1966, On the stability of the baroclinic circular vortex : a sufficient criterion for instability, *J. Atmo. Sci*. **23** 43.

Proudman J 1916, On the motion of solids in a liquid possessing vorticity, *Proc. R. Soc. Lond.* **A93** 92.

Rott N 1959, On the viscous core of a line vortex II, *Z. angew. Math. Phys*. **9b** 543.

Sullivan R D 1959, A two-cell vortex solution of the Navier-Stokes equation, *J. Aerosp. Sci*. **26** 767.

Sundqvist H 1970, Numerical simulation of the development of tropical cyclones with a ten-level model. Part I, *Tellus* **22** 359.

Takahashi K 2014a, Non-Eulerian inviscid vortices, *Fac. Lib. Arts Rev.* (*Tohoku Gakuin Univ.*) **167** 43 [http://www.tohoku-gakuin.ac.jp/research/journal/bk2014/pdf/no01_04.pdf].

Takahashi K 2014b, Classification of the steady axisymmetric vortices, *Fac. Lib. Arts Rev.* (*Tohoku Gakuin Univ.*) **168** 51 [http://www.tohoku-gakuin.ac.jp/research/journal/bk2014/pdf/no06_03.pdf].

Takahashi K 2015a, Simple vortices and typhoon, *Fac. Lib. Arts Rev.* (*Tohoku Gakuin Univ.*) **171** 105 (in Japanese) [http://www.tohoku-gakuin.ac.jp/research/journal/bk2015/pdf/no06_06.pdf] ; Erratum *Fac. Lib. Arts Rev.* (*Tohoku Gakuin Univ.*) **173** 144 (in Japanese) [http://www.tohoku-gakuin.ac.jp/ research/journal/bk2016/pdf/no02_05.pdf].

Takahashi K 2015b, On the non-existence of steady vortex solution with boundary surfaces, *J. Human Infom*. **20** 39 (in Japanese) [http://www.ipc.tohoku-gakuin.ac.jp/ghi/kenkyujyo/kiyou/ronbun/no20/ no20_takahashi.pdf].

Taylor G I 1917, Motion of solids in fluids when the flow is irrotational, *Proc. R. Soc. Lond*. **A93** 92.

Lib. Arts Rev. (*Tohoku Gakuin Univ.*) 2017, **176** 39-61.